Cancer Immunol Immunother (2006) 55: 797–807
DOI 10.1007/s00262-005-0068-8

ORIGINAL ARTICLE

Irma M. Sainz · Irma Isordia-Salas
Ricardo G. Espinola · Walter K. Long
Robin A. Pixley · Robert W. Colman

Multiple myeloma in a murine syngeneic model:modulation of growth and angiogenesis by a monoclonal antibody to kininogen

Received: 25 April 2005 / Accepted: 23 June 2005 / Published online: 27 September 2005

Abstract Multiple myeloma (MM), a B-cell malignancy characterized by proliferation of monoclonal plasma cells remains incurable. Murine plasma cell tumors share common features with human MM. We used two cell lines (B38 and C11C1) derived from P3X63Ag8 myeloma cells. The new cell lines were implanted subcutaneously in the strain of origin (Balb/c mice) and used as a model to monitor the effects of C11C1 monoclonal antibody (mAb) to kininogen (HK). We assessed their behavior by intraperitoneal and subcutaneous implantation, by implanting them together and by treating B38–MM with purified mAb C11C1. We evaluated growth, microvascular density (MVD), and cellular expression of urokinase-type plasminogen activator-receptor (uPAR), fibroblast growth factor-2 (FGF-2), vascular endothelial growth factor (VEGF), bradykinin-1 receptor (B1R), bradykinin-2 receptor (B2R) and HK. We found that both MM-cell-lines are uPAR positive, that mAb C11C1 inhibits its own tumor growth in vivo, slows down B38-MM growth rate when both MM are implanted together and when mAb C11C1 is injected intraperitoneally. MAb C11C1-treated-MM showed decreased MVD and HK binding in vivo without FGF-2, B1R or B2R expression changes. We propose that the B38-extramedullary-myeloma-model is a useful tool to study the interactions of this hematopoietic tumor and its environment and that mAb C11C1 may improve the efficacy of conventional MM treatment with minimal side effects.

Keywords Angiogenesis · Antiangiogenic-antibody · Bradykinin · Kininogen · Multiple myeloma · Plasmacytoma

Financial support: NIH grants. R01 CA-083121-08 (R.W.C.) and T32 HL-07777-14 (R.W.C.)

I. M. Sainz · I. Isordia-Salas · R. G. Espinola · W. K. Long
R. A. Pixley · R. W. Colman (✉)
The Sol Sherry Thrombosis Research Center,
Temple University School of Medicine,
3400 North Broad Street,
Philadelphia, PA, 19140 USA
E-mail: colmanr@temple.edu
Tel.: +1-215-7074665
Fax: +1-215-7072783

W. K. Long
Department of Microbiology and Immunology,
Temple University School of Medicine,
3400 North Broad Street, Philadelphia, PA, 19140 USA

Introduction

Multiple myeloma (MM) is a B-cell malignancy characterized by the accumulation of monoclonal immunoglobulin-secreting plasma cells in the bone marrow compartment, accompanied by osteoclastic bone destruction and severe pain [1]. Although MM is usually confined to the bone-marrow, related organ or tissue impairment, or end-organ damage may occur at the time of diagnosis or in the course of the disease [2]. Extramedullary (EM) involvement may occur in association with MM or as an isolated EM (extraosseous) plasmacytoma. EM involvement and/or solitary extraosseous plasmacytomas are rare diseases with an aggressive course. Response to conventional chemotherapy, thalidomide and/or high-dose therapy is poor, justifying the development of new therapeutic approaches [3]. Murine plasma cell tumors share a number or common features with human MM, suggesting their possible use as a model for this disease. However, one major difference between the two is the peritoneal localization of murine tumors as opposed to bone marrow residence of malignant plasma cells in early stages of human MM [4]. We propose the localized use of two cell lines derived from secretor myeloma P3X63Ag8 cells implanted in the strain of origin (Balb/c mice) as a model to monitor the disease behavior and its response to possible therapeutic approaches. We used two cell lines derived from P3X63Ag8 myeloma cells known as C11C1 and B38. The C11C1 and B38 MM cell lines were implanted intraperitoneally (IP) to confirm their malignant behavior. We used subcutaneous implantation thereafter

to assess the biological response of MM to a treatment with a monoclonal antibody (mAb) proven to inhibit angiogenesis [5].

P3X63Ag8 cells were fused with BALB/c spleen cells, from mice immunized against human plasma factor V. The new cell line known as B38-MM (hybridoma) secretes IgG_1 immunoglobulin against human factor V (FV) and cross-reacts with mouse FV protein [6]. When implanted intraperitoneally, this cell line spreads and grows killing the host. A second line was formed by fusing the P3X63Ag8 cells with Balb/c mice spleen cells from mice immunized against human plasma high-molecular-weight kininogen. The new cell line known as C11C1–MM (hybridoma) secretes IgG_1 immunoglobulin against domain 5 of human high molecular weight kininogen (HKD5) and cross-reacts with mouse HKD5 [5, 7]. We discovered that although C11C1-MM cells grow very well in vitro, they grow very slowly when implanted intraperitoneally, and the host mice show neither signs nor symptoms of MM.

We have demonstrated that mAb C11C1 inhibits the growth and decreases the vascularity of human tumors transplanted into immunodeficient (nude) mice [5]. In order to avoid the possible confounding effects of a competent immune system and the cross-species variable, we designed a multistep protocol using Balb/c mice as recipients of tumor cells from a hematologic malignancy, the B38-MM (derived from a Balb/c mouse secretory myeloma).

Materials and methods

Multiple Myeloma Cell Lines

C11C1 and B38 MM cell lines of Balb/c mouse origin, and mAb C11C1 were prepared and purified as previously described [6, 7].

To assess the intrinsic growth of each MM cell line in vitro, we plated out 5 ml of Dulbecco's modified Eagle medium (Invitrogen, Grand Island, NY, USA) containing 1×10^5 of either C11C1 or B38 cells per ml, per flask in 25 cm^2 flasks (x3). Cell counts from each flask were performed at 48, 72 and 96 h. Cell viability was determined by Trypan blue exclusion.

Animals

The functional immune system of syngeneic Balb/c mice and tumor cells of the same origin allowed the assessment of tumor growth in an immunocompetent environment and excluded the possibility of histocompatibility rejection. Female mice (8–10 weeks old) in groups of 3 or 5 per cage were housed in the animal facilities at Temple University and had free access to food and water. Research protocols were carried on under the guidelines of Temple's institutional animal care and use committee (IACUC). In all protocols, the animals were selected randomly and euthanized by an overdose of CO_2 inhalation.

Animal protocols

Protocol I: Intraperitoneal Multiple Myeloma cell implantation

To confirm the fact that C11C1-MM and B38 MM cell lines follow the usual growth pattern in vivo, ten Balb/c female mice (8–10 weeks old) received 0.5 ml of pristane IP (Sigma Biochemicals, Milwaukee, WI, USA). Ten days later the mice were divided in two groups of 5 mice each. B38-MM or C11C1-MM cells were injected IP (5×10^6 cells/mouse) to induce tumor growth. The experimental groups were checked every other day. The B38 group was euthanized on day 10, when tumor growth induced maximum abdominal distension (as required by protocol guidelines). Two C11C1 mice were euthanized on day 10 post-implantation to compare intraperitoneal tumor growth. At necropsy, ascitic fluid was collected and measured; and the abdominal contents were removed and fixed in 10% buffered formalin (Fisher Scientific, Fair Lawn, NJ, USA). The two C11C1 mice did not show any gross intraperitoneal myelomatous growth or ascites production. The remaining C11C1 mice ($n=3$) did not develop any ascites at any time and they were euthanized on day 28 post-cell implantation. At this time, the abdominal contents were removed and fixed in 10% buffered formalin.

Protocol II: Subcutaneous Multiple Myeloma cell implantation

To allow longer evolution of the MM-tumor growth in an accessible location that would facilitate the measurement and comparison of their volumes and in vivo growth, 34 female Balb/c mice (8–10 weeks old) were divided in three groups: negative control ($n=4$), B38 ($n=10$) and C11C1 ($n=20$). We used one-tenth the cell concentration than in protocol I. The back of each mouse was shaved to inject 5×10^5 cells subcutaneously in Hanks solution (HBSS; Sigma Biochemicals), with the exception of the negative control group, which received only HBSS. Mice were examined at least once a week recording the length, width and height of any developing tumors. We calculated the total volume of the tumors by the largest (a) and the smallest (b) superficial diameters: $V=(a\times b^2)/2$ [8]. When one or more tumors within group B38 reached the maximum length of 2 cm on day 11, the group was euthanized (as determined by protocol guidelines). At that time, no mice from the C11C1 group had reached the size limit; therefore, one out of four C11C1 cages (with five mice each) was randomly chosen and euthanized along with group B38. We monitored the 19 remaining mice from groups C11C1 (15 mice) and negative control (4 mice) for tumor growth for a total of 6 months after tumor implantation.

Protocol III: Subcutaneous Multiple Myeloma cell implantation, combined growth

Since C11C1-MM tumor cells did not grow as well in-vivo as it did in vitro, we decided to test its effect when implanted together with another MM cell line that did grow well in vivo and in vitro (B38-MM).

We shaved the backs of 20 female Balb/c mice (8–10 weeks old), and segregated them in four groups. A combined-cell group ($n=5$) received C11C1-MM (2×10^5) and B38-MM (2×10^5) hybridoma cells mixed together and suspended in 0.2 ml HBSS. We injected the cell mixture in the left back of each mouse (a total of 4×10^5 cells per mouse). A negative control group ($n=5$) received 0.2 ml of HBSS in the left back. A C11C1 group ($n=5$), received C11C1-MM 2×10^5 cells in the left back and a B38 group ($n=5$), received 2×10^5 B38-MM cells in the left back. The tumor growth in these experimental groups was monitored every other day until one or more tumors in any group reached the maximum length of 2 cm (as determined by protocol guidelines) on day 42 post-implantation.

Protocol IV: Subcutaneous Multiple Myeloma cell implantation, early vs. late treatment

To evaluate the effect of mAb C11C1 in syngeneic tumor prevention and treatment, 15 female Balb/c mice (8–10 weeks old) were separated into two initial groups, an early-treatment group ($n=6$) and a positive control group ($n=9$). On day 18, the positive control group was subdivided into positive control group ($n=3$) and late-treatment group ($n=6$):

(1) Early-treatment group, ($n=6$) received 2×10^5 B38-MM cells in 0.2 ml HBSS in the left back and were treated with 320 μg of purified mAb C11C1 suspended in 0.32 ml of HBSS IP every 48 h for 36 days starting on day 0.
(2) Positive control group ($n=9$) received 2×10^5 B38-MM cells suspended in 0.2 ml of HBSS implanted in the left back to monitor the unimpeded tumor growth
(3) On day 18, when one or more tumors within the positive control group ($n=9$) reached the predetermined length of 1.5 cm, this group was subdivided into late-treatment group ($n=6$) and positive control group ($n=3$). The late-treatment group started therapy similar to the early-treatment group (with 320 μg of purified mAb C11C1 IP every 48 h). Such treatment continued until tumors in the positive control group ($n=3$) reached the maximum length of 2.0 cm (in at least one mouse within the group).

Histology and immunochemistry processing

Tumor tissue was preserved in 10% buffered formalin and processed for paraffin embedding following the protocols supplied by B.D. Pharmingen 2000 (San Diego, CA, USA). We followed Biogenex immunoperoxidase procedure (San Ramon, CA, USA). Antimouse-uPAR antibody (Santa Cruz Biotechnology, Santa Cruz, CA, USA) was used to assess uPAR expression in C11C1 and B38 MM in protocol I. Tumor sections from protocols I, II, and IV were incubated with anti-mouse CD31 (PECAM; mAb ER-MP12; BMA, Peninsula Labs, San Carlos CA, USA) and anti-human von Willebrand Factor (vWF; Dako Cytomation, Carpinteria CA, USA), which cross-reacts with the mouse molecule. These two antibodies were used to highlight blood vessels. In protocol IV, we used the following antibodies: anti-HK [5] (Sigma Genosys Biotechnology, Woodlands, TX, USA), anti-VEGF, (that recognizes multiple VEGF isoforms) and anti-B2R (from Research Diagnostics, Flanders, NJ, USA), anti-B1R (Santa Cruz Biotechnology), and anti-FGF-2 (also known as basic FGF, bFGF), (Abcam Inc; Cambridge, MA, USA) to assess their corresponding antigen expression in harvested tumors (protocol IV).

Microvasculature density (MVD) assessment

We used a modification of the methods proposed by Bosari [9] and Vermeulen [10]. Briefly, digitalized images from ten high power fields (×400) per tumor (hot spots) were analyzed using Image-Pro-Plus 4.1 software (Media Cybernetics, Silver Spring, MD, USA). The evaluation was limited to those vessels with a cross-sectional area ranging from 10 to 50 μm. The total tumor surface area examined, the total number of vessels, and their surface area were tabulated to determine the mean number of vessels per square millimeter per group and the percentage of total area occupied by vessels (vessel area/total area × 100).

Immunohistochemistry assessment

To assess the quantitative in vivo binding of HK on tumor-endothelial cells, the total number of vessels (>50 μm) present in three high-power fields (×200) per tumor were counted and the percentage of immuno-positive vessels tabulated (protocol IV).

To assess the quantitative in vivo expression of uPAR (protocol I), B1R, B2R, FGF-2, and VEGF on tumor and stromal cells (Protocol IV), the positive and negative cells present in ten high-power fields (×1000) were counted and the percentage tabulated.

Statistics

Data was collected and tabulated without knowledge of the specimens' background. Results were analyzed using Student's *t*-test and expressed as mean ± standard error of the mean (SEM).

Results

MM cell lines growth in vitro

We recorded the intrinsic in vitro growth of each MM cell line. Starting with 1×10^5 cells the growth was similar in both cell lines during the first 48 h (4.4 ± 0.3 vs. $4.4\pm0.2\times10^5$ cells/ml). Differences in growth between C11C1-MM ($19.4\pm0.5\times10^5$ cells/ml) and B38-MM ($9.8\pm0.2\times10^5$ cells/ml) was only significant at 96 h ($P<0.001$) when C11C1-MM cells grew faster. Cell viability in both cell lines, at all time points was greater than 90% which allowed us to assess the possibility of auto-toxic (autocrine) effect on the cells where the antibodies were produced.

In summary, the in vivo growth difference between C11C1-MM and B38-MM cells is not due to different intrinsic growth in vitro and since they both are able to grow. Neither antibody has any autocrine toxic effect on the cells.

Animal protocols

Protocol I: intraperitoneal Multiple Myeloma development (Fig. 1)

B38-MM implanted-mice were sacrificed on day 10 (when one or more mice were unable to move upon stimulation).Two milliliters (mean) of ascitic fluid was collected per mouse. Two mice from the C11C1-MM group were sacrificed at the same time and did not have signs of either ascitis production or gross tumor growth. The remaining three mice from group C11C1-MM did not show any abdominal distension by day 28 when they were sacrificed to evaluate abdominal tumor development. At necropsy, abdominal contents of group B38-MM displayed multiple, large, congested tumor nodules ranging in size from 0.2 to 0.8 cm (Fig. 1a) which completely surrounded the small bowel with seeding of mesentery and diaphragm. The abdominal contents from the three remaining mice from group C11C1-MM euthanized at day 28 showed few pale, small nodules ranging in size from 0.1 to 0.3 cm, focally localized to the small bowel mesentery (Fig. 1a). Microscopic examination revealed neoplastic plasma cells with varying degrees of differentiation. There were no inflammatory cell infiltrates suggestive of the occurrence of immune reaction. Both groups showed expression of uPAR in 100% of tumor cells (Table 1). Group B38-MM tumors sections showed 19.3 ± 2.2 vessels per mm^2 (Fig. 1b left) and the area occupied by the vessels was $4\pm0.5\%$ (Fig. 1b right). The few tumor nodules developed by group C11C1-MM had 6.8 ± 1.8 vessels per mm^2 (Fig. 1B left) with a percentage of area occupied of $1.4\pm0.4\%$ (Fig. 1B right). The B38-MM group had more vessels than the C11C1-MM group ($P=0.008$).

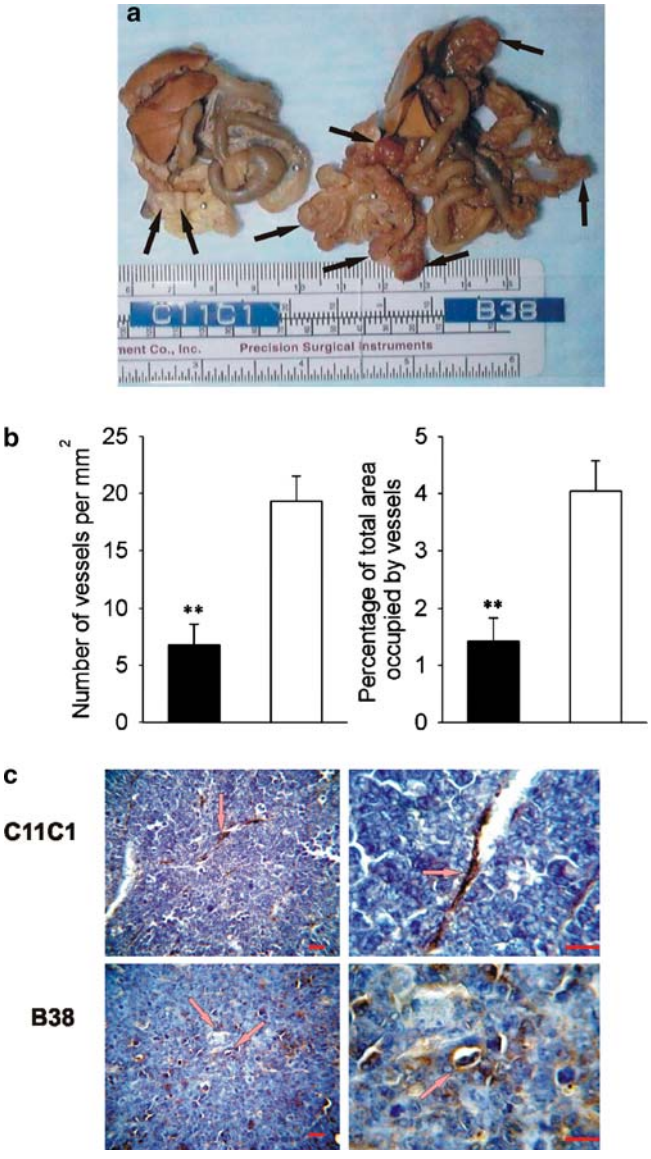

Fig. 1 Murine MM, intraperitoneal growth and microvascular density. **a**. IP growth. Representative gross abdominal findings at necropsy from specimens collected on maximum growth (B38-MM: day 10 and C11C1-MM: day 28). The *black arrows* point to the myelomatous growth in both specimens. C11C1 tumor nodules were clearly decreased in size and number. **b** Microvascular density (MVD) C11C1-MM *solid bars*; B38-MM *open bars*. The mean ± SEM number of vessels per mm^2 (left) and percentage of area occupied by vessels (right) in each group is shown. MVD was significantly decreased in sections from the C11C1-MM group ($n=3$) when compared to B38-MM group ($n=5$).**, $P=0.01$. **c** Immunohistochemistry of endothelial cells. Representative microphotographs (left: x400, right: x1000) from tumor sections showing blood vessel walls (*arrows*) stained golden-brown to black. The sections were incubated with an antibody to human vWF that crossreacts with the mouse molecule, and counterstained with hematoxylin. *Red bar* = 50 μm. C11C1-MM group has significantly fewer vessels than the B38-MM group

Representative microphotographs (×400 and ×1000) from sections stained with anti-vWF (that highlights the endothelial cells lining the vessels) are shown in Fig. 1c.

Table 1 Immunohistochemistry assessment of tissue immunopositivity in protocols I (MM intraperitoneal growth) and IV (early and late treatment of MM by IP injections of mAb C11C1)

Antibody	Experimental Groups			Cell Type
	PositiveControl	EarlyTreatment	LateTreatment	
	Percentage of Immunopositive Cells			
uPAR	100.0 ± 0.0	100.0 ± 0.0	100.0 ± 0.0	Tumor Cells
HK	77.8 ± 5.3	27.2 ± 1.8	42.3 ± 7.4	Endothelial Cells lining blood vessels
FGF-2	100 ± 0.0	100 ± 0.0	100 ± 0.0	Stromal and Tumor Cells
VEGF	5.2 ± 0.9	99.2 ± 0.1	99.1 ± 0.1	Stromal and Tumor Cells
B2R	100.0 ± 0.0	100.0 ± 0.0	100.0 ± 0.0	Stromal and Tumor Cells
B1R	0.0 ± 0.0	0.0 ± 0.0	0.0 ± 0.0	Stromal and Tumor Cells

uPAR urokinase type plaminogen activator receptor. *HK* high molecular weight kininogen. *FGF-2* fibroblast-growth-factor-2. *VEGF* vascular-endothelial-growth-factor. *B2R* bradykinin 2 receptor. *B1R* bradykinin 1 receptor

In summary, C11C1 tumors had a decreased incidence, a significantly slower growth in vivo, a smaller volume and a decreased MVD when compared to the B38-MM group.

Protocol II: Subcutaneous MM development (Fig. 2)

The negative control group did not show any spontaneous tumor growth ($n=4$; not plotted). Ten out of ten mice from group B38 developed tumors and were harvested on day 11 after implantation. In the case of C11C1 implanted mice 5 out of the 20 were euthanized on day 11. Two of these mice had tumor growth and were harvested. By day 11 a total of 7 tumors developed in the 20 mice implanted with C11C1 myeloma cells. The remaining five animals with tumors were allowed to progress; they regressed to a grossly undetectable size by day 22 (after implantation) and did not increase in size prior to termination of the observation period. There were no tumors present by macroscopic (gross) examination in any of the 15 remaining C11C1-implanted mice at necropsy (performed 6 months after tumor implantation). On day 11, the B38 group had a much greater mean tumor volume (174 ± 94 mm^3) than the C11C1 group (4.6 ± 2.9 mm^3) ($P=0.01$; Fig. 2a). Microscopic examination revealed neoplastic plasma cells with varying degrees of differentiation. There were no inflammatory cell-infiltrates suggestive of the occurence of immune reaction present. B38 tumors had 18.2 ± 1.6 vessels per mm^2 (Fig. 2b left) with $3.5 \pm 0.3\%$ of area occupied by vessels (Fig. 2b right). Tumors found in the mice from group C11C1 (sacrificed on day 11) had 8.7 ± 1.3 vessels per mm^2 (Fig. 2b left) and occupied $1.7 \pm 0.2\%$ of the tumor area (Fig. 2b right). B38 had more vessels per mm^2 and occupied more surface area than C11C1 tumors ($P=0.01$).

In summary, C11C1 tumors had significantly decreased incidence (7 tumors out of 20 mice), volume, and MVD than the B38 group. C11C1 tumors had slower growth in vivo and the five tumors allowed to progress (not excised), regressed to a grossly undetectable size.

Protocol III: Subcutaneous MM, combined growth (Fig. 3)

The negative control group did not show any spontaneous tumor growth (not plotted). C11C1 group showed negligible growth. The combined group had a biphasic growth pattern: it grew faster than the B38 group the first 10 days, decreased in size for the following 15 days,

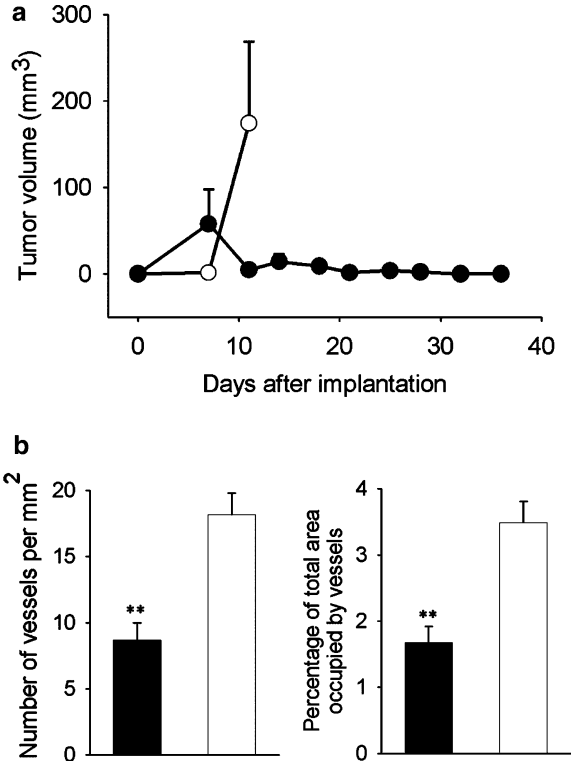

Fig. 2 Murine MM, subcutaneous growth and MVD. **a** Growth: Values shown are mean ± SEM. Group B38 (*open circles*) ($n=10$) reached the 2 cm length limit by day 11. C11C1 group (*solid circles*) ($n=20$) did not reach the length limit. The C11C1 tumors not excised regressed by day 22. Statistical comparisons made with day 11 data ($P=0.02$). **b** MVD C11C1 *solid bars*; B38 *open bars*. The mean ± SEM of the number of vessels per mm^2 (*left*) and the percentage of total area occupied by vessels (*right*) were statistically significant. $^{**}P=0.01$.

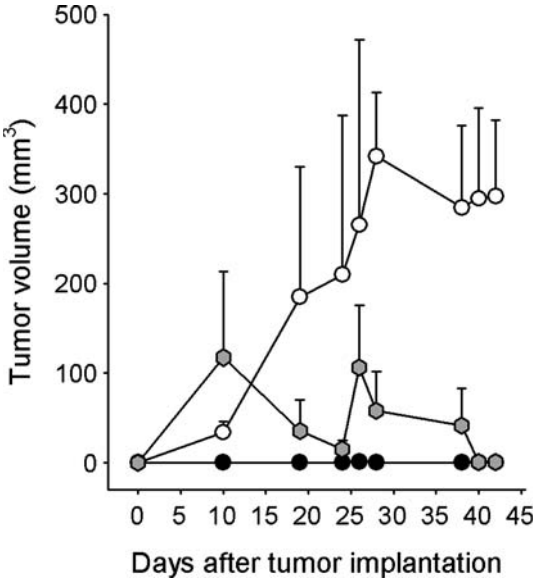

Fig. 3 Murine MM, combined subcutaneous growth: Combined group C11C1 and B38 (*gray hexagons*) received C11C1-MM and B38-MM cells which were implanted together in the back of Balb/c mice (n = 5) to monitor their growth. Group B38 (*open circles*) ($n = 5$) and group C11C1 (*solid circles*) ($n = 5$) received either B38-MM or C11C1-MM cells (implanted in the back of Balb/c mice) and were used to monitor their separate growth rate in vivo. There were no significant differences up to and included day 26 between the combined group and the B38 group. At day 28 and beyond the B38 group showed a statistically significant increase in volume when compared to the combined group ($P < 0.05$). The B38 group tumor volume was significantly larger than the C11C1 group from day 10 and beyond ($P < 0.05$). Values shown are mean ± SEM.

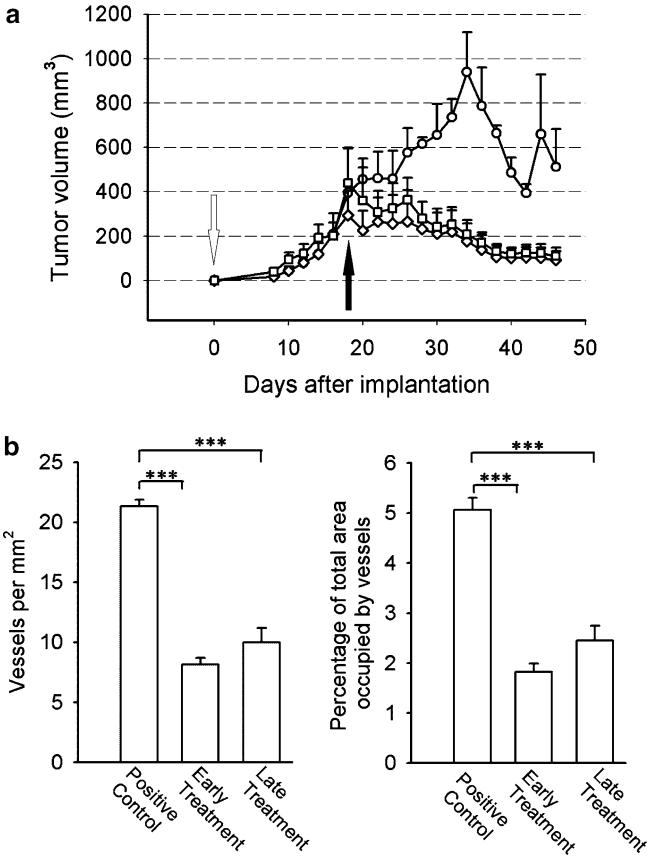

Fig. 4 Murine MM, subcutaneous growth and early and late treatment. **a** Growth: All animals were implanted with B38-MM cells. The untreated control group (circles) showed a steady growth rate until day 32. Animals that received purified mAb C11C1 for early treatment from day zero (*open arrow*; *diamonds*) showed a statistically significant decrease in tumor volume from the untreated control group starting from day 28 ($P < 0.05$). Animals from the late-treatment group started mAb C11C1 intraperitoneal injections on day 18 (*solid arrow*; *squares*) showed statistically significant decrease in tumor volume on day 30 and afterwards ($P < 0.05$). Values shown are mean ± SEM. **b** B38-MM early- and late-treatment MVD: The mean ± SEM of the number of vessels per mm^2 (*left*) and the percentage of total area occupied by vessels (*right*) were statistically significant between the control and both treatment groups ($P < 0.005$). There was no statistically significant difference between the treatment groups ($P = 0.01$). ***$P < 0.005$

grew again for the next 3 days, and then continued to steadily decrease for the remaining span of the experiment. The B38 group grew steadily during the monitoring period. The combined C11C1 and B38 group developed tumors in four out of five mice by day 10 after implantation and three of these tumors regressed to and undetectable size by day 42. There was only one grossly evident tumor (4.5 mm^3) present at necropsy (day 42 post-implantation). One mouse (out of five) from group C11C1 developed a tumor that reached a maximum volume of 3.3 mm^3 and regressed (not grossly evident at necropsy). The B38 group developed tumors in five out of five mice (297.4 ± 84.9 mm^3). When comparing the combined group (C11C1 + B38) with group B38, the difference in tumor volumes was statistically significant ($P < 0.02$) starting at day 28 post-implantation.

In summary, the growth of combined B38 and C11C1 cells was significantly decreased. Group B38 grew unimpeded and group C11C1 had a markedly decreased growth.

Protocol IV: Subcutaneous MM, early vs. late treatment (Fig. 4)

Tumors were palpable by day 8 in all specimens. They initially grew similarly in all groups. In the early-treatment group, (mAb C11C1 started on day zero) tumor growth started to decrease in size on day 19 similar to the tumor volume in the late-treatment group (started treatment on day 18). Both groups steadily decreased in size until necropsy (day 36 post-implantation). Statistically significant difference in tumor volumes was found on day 28 between the untreated-control and early-treatment groups ($P < 0.05$), and on day 30, between the control and late-treatment groups ($P < 0.05$). There was no statistically significant difference at any time in tumor volume between the treatment groups (Fig. 4a). Tumor weights at necropsy day (positive control group, 589.0 ± 56.2 mg; early-treatment group: 36.2 ± 14.4 mg; late-treatment-group, 123 ± 51.5 mg) were consistent with the final tumor volumes (positive control group, 511.9 ± 171.6 mm^3;

early-treatment group, 91.5 ± 41.2 mm^3; late-treatment-group, 109.1 ± 39.3 mm^3). Microscopic examination revealed neoplastic plasma cells with varying degrees of differentiation. There were no inflammatory cell-infiltrates suggestive of occurrence of immune reaction. Control tumors had 21.35 ± 0.52 vessels/mm^2 (Fig. 4b left) occupying $5.10 \pm 0.23\%$ of total tumor area assessed (Fig. 4b right). The early-treatment group (treatment initiated on day 0) had 8.12 ± 0.55 v/mm^2 and occupied $1.82 \pm 0.17\%$ of total area. The late-treatment group (treatment initiated on day 18 post-tumor cell implantation) had 9.99 ± 1.18 v/mm^2 and occupied $2.45 \pm 0.30\%$ of tumor area. The control group had more vessels per mm^2 (Fig. 4B left) than the treatment groups ($P < 0.001$); correspondingly, the control group vessels occupied more tumor area than in the treatment groups ($P < 0.001$) (Fig. 4b right). There was no significant difference between the experimental treatment groups either in vascular density or in percentage of area occupied by vessels.

Immunohistochemistry assessment (Table 1, Fig. 5)

The control group had higher HK expression on blood vessels than the treatment groups ($P < 0.005$). There was no significant difference in HK expression between the experimental treatment groups. FGF-2 expression was diffusely present in both, stromal and tumor cells in all groups. The control group had significantly less VEGF expression than the treatment groups ($P < 0.001$). There was no difference in VEGF expression between the experimental treatment groups. B2R expression was diffusely present in both, stromal and tumor cells in all groups, while B1R expression was not detected (absent).

In summary, C11C1 mAb injections slowed down the B38 MM cell growth, decreased microvascular density and HK in vivo binding to endothelial cells as effectively when given after the tumor had reached the predetermined size limit as when given since the time of implantation.

Discussion

Tumor growth and tumor angiogenesis involve several, seemingly different but intertwined pathways (Fig. 6a), and the findings in this report indicate a strong influence from the plasma Kallikrein–Kinin System (Fig. 6b). Although MM is a malignant tumor sensitive to chemotherapy and radiation therapy, the long-term disease-free survival is rare. We decided to study a cell line derived from a murine MM implanted in an extramedullary site and tried to mimic the natural evolution of the disease in an immunocompetent host. Thus, in this report, we used an animal model of a uPAR-positive murine multiple myeloma (B38-MM) in a syngeneic host (Balb/c mice). We confirmed B38-MM malignant behavior and assessed its growth, vascular density and response to mAb C11C1, a mAb against HKD5. We

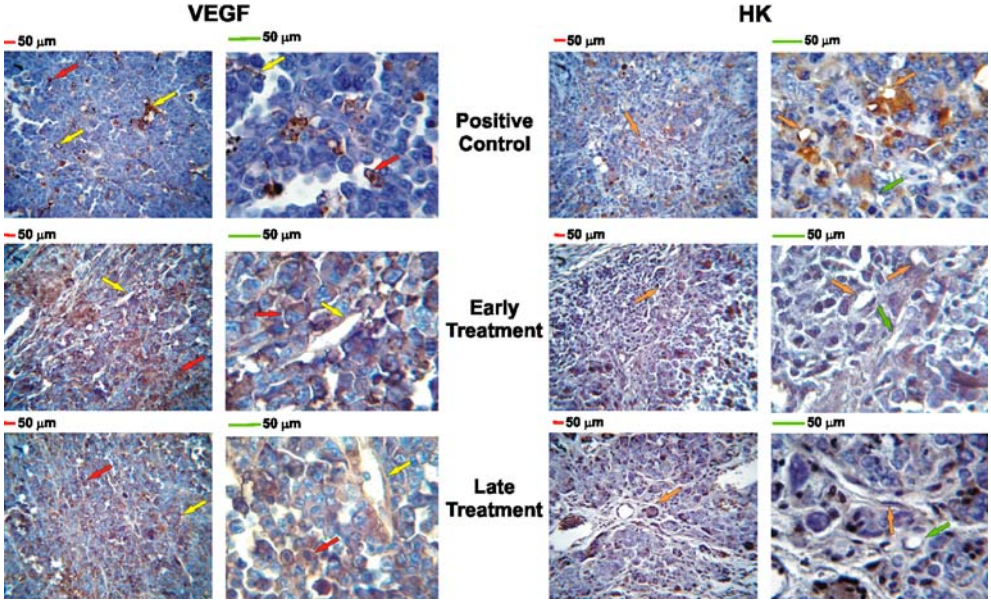

Fig. 5 VEGF and HK immunohistochemistry: magnification: left ×400, right ×1000; *red* and *green bars* = 50 micrometers; positive staining is indicated by brown pigment within cytoplasm. VEGF (*left panel*): *red arrows* point to malignant tumor cells; *yellow arrows* point to stromal tissue (connective tissue, endothelial cells); The positive control group showed $5.2 \pm 0.9\%$ of tumor and stromal cells positive to VEGF while both treatment groups showed more than 90% immunopositivity. HK (*right panel*): *orange arrows* point to HK-positive endothelial cells; *green arrows* point to HK-negative endothelial cells. The positive control group showed more than 75% of endothelial cell immunopositivity while both treatment groups showed significantly less HK-positive endothelial cells (early treatment: $27.2 \pm 1.8\%$; late treatment: $42.3 \pm 7.4\%$). There was no difference in immunopositivity for uPAR, FGF-2, BIR, and B2R among all experimental groups

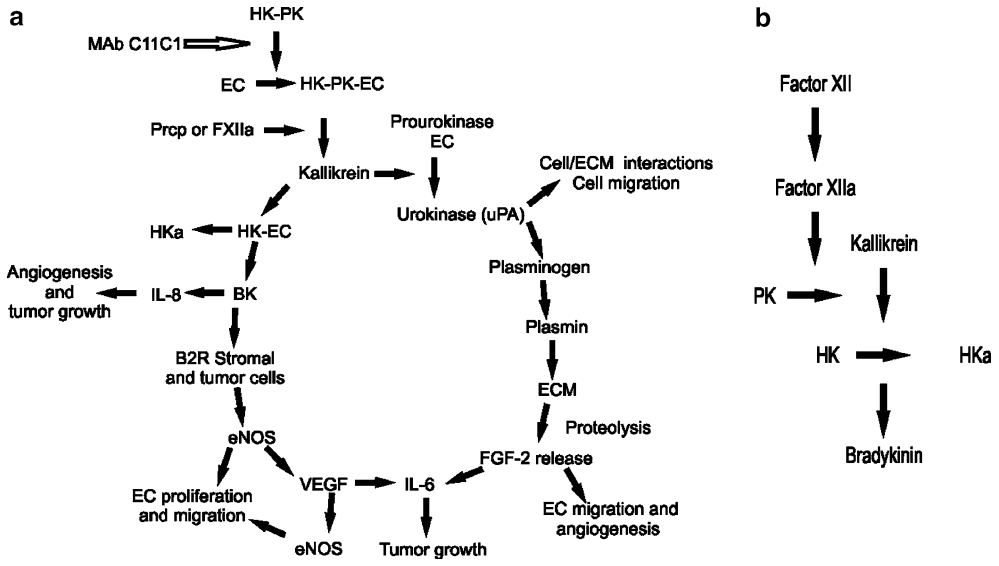

Fig. 6 The Plasma Kallikrein–Kinin System and mAb C11C1 effect in the angiogenic cascade. **a** C11C1 mAb and the angiogenic cascade. *MAb C11C1* C11C1 monoclonal antibody. *HK* high-molecular-weight kininogen. *PK* prekallikrein. *EC* endothelial cell. *Prcp* prolylcarboxypeptidase. *FXIIa* activated coagulation factor XII. *HKa* cleaved high-molecular-weight kininogen. *IL-8* interleukin 8. *BK* bradykinin. *B2R* bradykinin 2 receptor. *eNOS* endothelial cell nitric oxide system. *VEGF*: vascular endothelial growth factor. *IL-6* interleukin 6. *FGF-2* fibroblast growth factor 2, basic fibroblast growth factor. *ECM* extracellular matrix. *uPA* urokinase type plasminogen activator. The plasma complex HK–PK binds to the endothelial cells, where PK is activated to kallikrein (by either Prcp or FXIIa). Kallikrein cleaves HK releasing HKa and BK. BK stimulates IL-8 secretion (a potent angiogenic and tumor growth inducer) and the production and secretion of eNOS through the B2R on the surface of stromal and tumor cells. eNOS induces endothelial cell release of VEGF and endothelial cell proliferation and migration. VEGF induces eNOS and IL-6 release (which promotes tumor growth). Kallikrein also cleaves prourokinase to urokinase initiating a different pathway. Urokinase is involved in cell/ECM interactions favoring tumor spread and endothelial cell migration. Urokinase also activates plasminogen into plasmin and the proteolysis of the extracellular matrix releasing FGF-2. FGF-2 induces endothelial cell migration and the release of IL-6, which promotes tumor growth. MAb C11C1 inhibits the adhesion of HK and/ or the HK–PK complex to the endothelial cells, inhibiting the BK and uPA activation through kallikrein thus inhibiting tumor angiogenesis and growth. **b** Plasma Kallikrein-Kinin system: Consists of three proteins, Factor XII (*FXII*), Prekallikrein (*PK*), and high-molecular-weight kininogen (*HK*). Activated FXII (*FXIIa*) cleaves PK to kallikrein; kallikrein cleaves HK releasing BK and activated HK (*HKa*)

previously demonstrated that although mAb C11C1 has no effect on in vitro proliferation, it does inhibit the growth and angiogenesis in vivo of a human colon carcinoma (HCT-116) [5]. Our results indicate that the decrease in tumor growth is not due to an intrinsic decrease in the rate of tumor cell proliferation since the MM-secreting mAb C11C1 grows equally fast in vitro as those hybridomas secreting B38 mAb during the first 48 h, and faster by 96 h after plating. The antibody effect is not cytotoxic since cell viability in vitro was greater than 90%. In all protocols, C11C1 tumors grew slowly and when not excised, they regressed to an undetectable size. When comparing incidence and tumor volume, C11C1-MM implanted mice had a decreased incidence and tumor volume (in all protocols) than B38-MM implanted mice. In protocol I, B38-MM grew faster and followed the expected growth pattern of a murine myeloma (it spread throughout the abdominal cavity, involving both solid and hollow organs) (Fig. 1a). Quantitative evaluation of MVD (vessels/mm^2 and the percentage area occupied by vessels) in all protocols assessed (I, II and IV) was significantly decreased in the C11C1-MM group when compared to the B38-MM group (Figs. 1b, 2b and 4b).

In protocol III, we were able to demonstrate that mAb C11C1 had an in situ paracrine effect. MAb C11C1 significantly slowed the growth of B38-MM when they were implanted together (Fig. 3). In protocol IV, we demonstrated that purified mAb C11C1 was effective systemically in the treatment of B38-MM but it did not inhibit its early growth (Fig. 4a). We attribute the lag in effect of mAb C11C1 in the early-treatment group to the dependency on diffusion in the avascular phase of tumor growth [11] since C11C1-MM cells grow well in vitro. As expected, the groups treated with mAb C11C1 showed a significantly decreased MVD (Fig. 4b). In this protocol, we also assessed some of the growth factors associated with tumor growth such as FGF-2 and VEGF (Table 1, Fig. 5). Plasma cells from MM have been shown to produce FGF-2 [12, 13] and VEGF [14] as do the B38-MM cells. In the case of the latter, we found interesting results: the untreated group had rare VEGF expression ($5.17 \pm 0.87\%$) in both stromal and plasma cells while both treated groups showed more than 99% expression (stromal and plasma cells). How can we explain the increase in VEGF expression in the treated groups? There are multiple regulatory pathways of VEGF expression [15–18]. Thus, one possible expla-

nation is that the VEGF expression seen in the treatment groups may be secondary to hypoxia pathways. Since our treatment interfered with the pathways of BK stimulation of VEGF production and secretion (Fig. 6a), and although such interference was enough to decrease vascular and tumor cell proliferation, it did not block the pathways regulated by hypoxia [19].

FGF2 has a complex role in tumor development, it induces endothelial cell proliferation, migration and angiogenesis in vitro [20]. FGF-2 regulates the expression of several molecules that mediate critical steps during angiogenesis including interstitial collagenase, uPA, plasminogen activator inhibitor (PAI-1), uPA receptor (uPAR), and β1 integrins [21, 22].

Expression of the BK receptors, B1R [23, 24] and B2R [25, 26] have been identified in different clinical cancer specimens and murine tumor and stromal tissues. In our MM model, B1R expression was absent in all experimental groups while B2R was diffusely positive in B38 myeloma cells.

Finally we compared HK in vivo binding among the three groups. As expected HK staining was significantly decreased in both experimental treatment groups, since mAb C11C1 blocks HK binding to endothelial cells. These results are similar to our findings in human colon carcinoma specimens from mAb C11C1-treated nude mice [5].

A central focus in the pathophysiology of MM is the complex interactive network between MM cells and their environment [27], including regulatory pathways and interactions among adhesion molecules and cytokines, which support the growth of malignant plasma cells, protect them from apoptosis and contribute to their neovascularization (Fig. 6a). We and other laboratories have reported that HK induces angiogenesis through BK release [28, 29]. HK binds to endothelial cell membranes through an interaction with a multiprotein receptor complex comprising cytokeratin-1, a receptor of the q-subunit of the complement first component (gC1qR) and uPAR [30]. The ligation of this receptor complex regulates the assembly and activation of the plasma kallikrein–kinin system (Fig. 6b) and enhances the conversion of prourokinase to urokinase by kallikrein, as well as cell-associated fibrinolysis by plasmin [31]. We have shown that C11C1 binds to the epitope in HKD5 [7] preventing HK binding to the endothelial cell surface [5] and blocking HK proteolysis, inhibiting the release of angiogenic BK [28].

Our approach interferes with at least two angiogenic and tumor growth-induction pathways, BK, and the uPA/uPAR system [32, 33]. Thus, we propose that the model of B38-MM provides a useful tool to study the interactions of this hematopoietic tumor and its environment in an accessible area, in an immunocompetent host. We also postulate that by blocking HK binding to the endothelial cells, we inhibit the production of kallikrein, BK and urokinase. Decrease of kallikrein will result in decrease of BK (from cleaved HK) and urokinase (from prourokinase). Lower levels of BK will also result in decreased stimulation of the nitric oxide system (NOS) pathway [34, 35], which is involved in the production and secretion of VEGF [36]. There have been reports of BK stimulating the production of a chemokine, interleukin 8 [37] which is also considered a potent angiogenic and tumor growth inducer [38–41]. Decrease in urokinase will result in decrease in the production of plasmin that proteolyses fibrinogen and stimulates the secretion of FGF-2 [42, 43]. Furthermore, the uPA/uPAR system is involved in cell/ECM interactions and regulates cell migration [44, 45]. The decrease in the secretion of VEGF and fibrinogen proteolysis [46] by these pathways will decrease both, tumor cell proliferation and angiogenesis.

We have tested the effects of mAb C11C1 in the three main histological types of tumors: a human sarcoma (HT-1080) [47]; a human epithelial carcinoma (HCT-116) [5]; and a hematologic malignancy (B38 murine multiple myeloma). Supported by our results, we suggest that the use of mAb C11C1 as an antiangiogenic treatment in combination with conventional cytotoxic, radiation or immunotherapy may improve the efficacy of these anticancer therapies by decreasing the tumor burden. Furthermore, the reported patients with known kininogen deficiencies are asymptomatic and long-lived [48] thus HK inhibition by this selective mAb would have minimal adverse side effects.

References

1. Hideshima T, Anderson KC (2002) Molecular mechanisms of novel therapeutic approaches for multiple myeloma. Nat Rev Cancer 2:927–937
2. Criteria for the classification of monoclonal gammopathies, (2003) multiple myeloma and related disorders: a report of the International Myeloma Working Group. Br J Haematol 121:749–57
3. Damaj G, Mohty M, Vey N, Dincan E, Bouabdallah R, Faucher C, Stoppa AM, Gastaut JA (2004) Features of extramedullary and extraosseous multiple myeloma: a report of 19 patients from a single center. Eur J Haematol 73:402–406
4. Roschke V, Hausner P, Kopantzev E, Pumphrey JG, Riminucci M, Hilbert DM, Rudikoff S (1998) Disseminated growth of murine plasmacytoma: similarities to multiple myeloma. Cancer Res 58:535–541
5. Song JS, Sainz IM, Cosenza SC, Isordia-Salas I, Bior A, Bradford HN, Guo YL, Pixley RA, Reddy EP, Colman RW (2004) Inhibition of tumor angiogenesis in vivo by a monoclonal antibody targeted to domain 5 of high molecular weight kininogen. Blood 104:2065–2072
6. Annamalai AE, Stewart GJ, Hansel B, Memoli M, Chiu HC, Manuel DW, Doshi K, Colman RW (1986) Expression of factor V on human umbilical vein endothelial cells is modulated by cell injury. Arteriosclerosis 6:196–202
7. Schmaier AH, Schutsky D, Farber A, Silver LD, Bradford HN, Colman RW (1987) Determination of the bifunctional properties of high molecular weight kininogen by studies with monoclonal antibodies directed to each of its chains. J Biol Chem 262:1405–1411
8. Carlsson G, Gullberg B, Hafstrom L (1983) Estimation of liver tumor volume using different formulas - an experimental study in rats. J Cancer Res Clin Oncol 105:20–23
9. Bosari S, Lee AK, DeLellis RA, Wiley BD, Heatley GJ, Silverman ML (1992) Microvessel quantitation and prognosis in invasive breast carcinoma. Hum Pathol 23:755–761

10. Vermeulen PB, Gasparini G, Fox SB, Toi M, Martin L, McCulloch P, Pezzella F, Viale G, Weidner N, Harris AL, Dirix LY (1996) Quantification of angiogenesis in solid human tumours: an international consensus on the methodology and criteria of evaluation. Eur J Cancer 32A:2474–2484
11. Folkman J (1974) Tumor angiogenesis. Adv Cancer Res 19:331–358
12. Bisping G, Leo R, Wenning D, Dankbar B, Padro T, Kropff M, Scheffold C, Kroger M, Mesters RM, Berdel WE, Kienast J (2003) Paracrine interactions of basic fibroblast growth factor and interleukin-6 in multiple myeloma. Blood 101:2775–2783
13. Vacca A, Ribatti D, Presta M, Minischetti M, Iurlaro M, Ria R, Albini A, Bussolino F, Dammacco F (1993) Bone marrow neovascularization, plasma cell angiogenic potential, and matrix metalloproteinase-2 secretion parallel progression of human multiple myeloma. Blood 93:3064–3073
14. Kumar S, Witzig TE, Timm M, Haug J, Wellik L, Fonseca R, Greipp PR, Rajkumar SV (2003) Expression of VEGF and its receptors by myeloma cells. Leukemia 17:2025–2031
15. Shweiki D, Itin A, Soffer D, Keshet E (1992) Vascular endothelial growth factor induced by hypoxia may mediate hypoxia-initiated angiogenesis. Nature 359:843–845
16. Gardner AM, Olah ME (2003) Distinct protein kinase C isoforms mediate regulation of vascular endothelial growth factor expression by A2A adenosine receptor activation and phorbol esters in pheochromocytoma PC12 cells. J Biol Chem 278:15421–15428
17. Knox AJ, Corbett L, Stocks J, Holland E, Zhu YM, Pang L (2001) Human airway smooth muscle cells secrete vascular endothelial growth factor: up-regulation by bradykinin via a protein kinase C and prostanoid-dependent mechanism. FASEB J 15:2480–2488
18. Mukhopadhyay D, Knebelmann B, Cohen HT, Ananth S, Sukhatme VP (1997) The von Hippel-Lindau tumor suppressor gene product interacts with Sp1 to repress vascular endothelial growth factor promoter activity. Mol Cell Biol 17:5629–5639
19. Mazure NM, Chen EY, Laderoute KR, Giaccia AJ (1997) Induction of vascular endothelial growth factor by hypoxia is modulated by a phosphatidylinositol 3-kinase/Akt signaling pathway in Ha-ras-transformed cells through a hypoxia inducible factor-1 transcriptional element. Blood 90:3322–3331
20. Basilico C, Moscatelli D (1992) The FGF family of growth factors and oncogenes. Adv Cancer Res 59:115–165
21. Mignatti P, Rifkin DB (1993) Biology and biochemistry of proteinases in tumor invasion. Physiol Rev 73:161–195
22. Klein S, Giancotti FG, Presta M, Albelda SM, Buck CA, Rifkin DB (1993) Basic fibroblast growth factor modulates integrin expression in microvascular endothelial cells. Mol Biol Cell 4:973–982
23. Taub JS, Guo R, Leeb-Lundberg LM, Madden JF, Daaka Y (2003) Bradykinin receptor subtype 1 expression and function in prostate cancer. Cancer Res 63:2037–2041
24. Barki-Harrington L, Bookout AL, Wang G, Lamb ME, Leeb-Lundberg LM, Daaka Y (2003) Requirement for direct cross-talk between B1 and B2 kinin receptors for the proliferation of androgen-insensitive prostate cancer PC3 cells. Biochem J 371:581–587
25. Wu J, Akaike T, Hayashida K, Miyamoto Y, Nakagawa T, Miyakawa K, Muller-Esterl W, Maeda H (2002) Identification of bradykinin receptors in clinical cancer specimens and murine tumor tissues. Int J Cancer 98:29–35
26. Ikeda Y, Hayashi I, Kamoshita E, Yamazaki A, Endo H, Ishihara K, Yamashina S, Tsutsumi Y, Matsubara H, Majima M (2004) Host stromal bradykinin B2 receptor signaling facilitates tumor-associated angiogenesis and tumor growth. Cancer Res 64:5178–5185
27. Hideshima T, Chauhan D, Podar K, Schlossman RL, Richardson P, Anderson KC (2001) Novel therapies targeting the myeloma cell and its bone marrow microenvironment. Semin Oncol 28:607–612
28. Zhao Y, Qiu Q, Mahdi F, Shariat-Madar Z, Rojkjaer R, Schmaier AH (2001) Assembly and activation of HK-PK complex on endothelial cells results in bradykinin liberation and NO formation. Am J Physiol Heart Circ Physiol 280:H1821–H1829
29. Hayashi I, Amano H, Yoshida S, Kamata K, Kamata M, I-nukai M, Fujita T, Kumagai Y, Furudate S, Majima M (2002) Suppressed angiogenesis in kininogen-deficiencies. Lab Invest 82:871–880
30. Colman RW, Pixley RA, Najamunnisa S, Yan W, Wang J, Mazar A, McCrae KR (1997) Binding of high molecular weight kininogen to human endothelial cells is mediated via a site within domains 2 and 3 of the urokinase receptor. J Clin Invest 100:1481–1487
31. Mahdi F, Shariat-Madar Z, Kuo A, Carinato M, Cines DB, Schmaier AH (2004) Mapping the interaction between high molecular mass kininogen and the urokinase plasminogen activator receptor. J Biol Chem 279:16621–16628
32. Rakic JM, Maillard C, Jost M, Bajou K, Masson V, Devy L, Lambert V, Foidart JM, Noel A (2003) Role of plasminogen activator-plasmin system in tumor angiogenesis. Cell Mol Life Sci 60:463–473
33. Mondino A, Blasi F (2004) uPA and uPAR in fibrinolysis, immunity and pathology. Trends Immunol 25:450–455
34. Venema VJ, Marrero MB, Venema RC (1996) Bradykinin-stimulated protein tyrosine phosphorylation promotes endothelial nitric oxide synthase translocation to the cytoskeleton. Biochem Biophys Res Commun 226:703–710
35. Harris MB, Ju H, Venema VJ, Liang H, Zou R, Michell BJ, Chen ZP, Kemp BE, Venema RC (2001) Reciprocal phosphorylation and regulation of endothelial nitric-oxide synthase in response to bradykinin stimulation. J Biol Chem 276:16587–16591
36. Papapetropoulos A, Garcia-Cardena G, Madri JA, Sessa WC (1997) Nitric oxide production contributes to the angiogenic properties of vascular endothelial growth factor in human endothelial cells. J Clin Invest 100:3131–3139
37. Hayashi R, Yamashita N, Matsui S, Fujita T, Araya J, Sassa K, Arai N, Yoshida Y, Kashii T, Maruyama M, Sugiyama E, Kobayashi M (2000) Bradykinin stimulates IL-6 and IL-8 production by human lung fibroblasts through ERK- and p38 MAPK-dependent mechanisms. Eur Respir J 16:452–458
38. Smith DR, Polverini PJ, Kunkel SL, Orringer MB, Whyte RI, Burdick MD, Wilke CA, Strieter RM (1994) Inhibition of interleukin 8 attenuates angiogenesis in bronchogenic carcinoma. J Exp Med 179:1409–1415
39. Arenberg DA, Kunkel SL, Polverini PJ, Glass M, Burdick MD, Strieter RM (1996) Inhibition of interleukin-8 reduces tumorigenesis of human non-small cell lung cancer in SCID mice. J Clin Invest 97:2792–2802
40. Yuan A, Chen JJ, Yao PL, Yang PC (2005) The role of interleukin-8 in cancer cells and microenvironment interaction. Front Biosci 10:853–865
41. Tobler A, Moser B, Dewald B, Geiser T, Studer H, Baggiolini M, Fey MF (1993) Constitutive expression of interleukin-8 and its receptor in human myeloid and lymphoid leukemia. Blood 82:2517–2525
42. Jonca F, Ortega N, Gleizes PE, Bertrand N, Plouet J (1997) Cell release of bioactive fibroblast growth factor 2 by exon 6-encoded sequence of vascular endothelial growth factor. J Biol Chem 272:24203–24209
43. Ribatti D, Leali D, Vacca A, Giuliani R, Gualandris A, Roncali L, Nolli ML, Presta M (1999) in vivo angiogenic activity of urokinase: role of endogenous fibroblast growth factor-2. J Cell Sci 112 (Pt 23):4213–4221
44. Ossowski L, Clunie G, Masucci MT, Blasi F (1991) in vivo paracrine interaction between urokinase and its receptor: effect on tumor cell invasion. J Cell Biol 115:1107–1112
45. Chapman HA (1997) Plasminogen activators, integrins, and the coordinated regulation of cell adhesion and migration. Curr Opin Cell Biol 9:714–724

46. Nehls V, Herrmann R (1996) The configuration of fibrin clots determines capillary morphogenesis and endothelial cell migration. Microvasc Res 51:347–364
47. Colman RW, Pixley RA, Sainz IM, Song JS, Isordia-Salas I, Muhamed SN, Powell JA, Jr Mousa SA (2003) Inhibition of angiogenesis by antibody blocking the action of proangiogenic high-molecular-weight kininogen. J Thromb Haemost 1:164–170
48. Colman RW (1992) Contributions of Mayme Williams to the elucidation of the multiple functions of plasma kininogens. Thromb Haemost 68:99–101